Inter- and Intramolecular Excited-State Interactions of Surfactant-Active Rhenium(I) Photosensitizers†

G. A. Reitz,‡ J. N. Demas,*,‡ B. A. DeGraff,*,§ and Eileen M. Stephens‖

Contribution from the Department of Chemistry, University of Virginia, Charlottesville, Virginia 22901, Department of Chemistry, James Madison University, Harrisonburg, Virginia 22807, and Department of Physiology, School of Medicine, University of Virginia, Charlottesville, Virginia 22901. *Received November 9, 1987*

Abstract: A new series of surfactant-active complexes of the form $[(bpy)Re(CO)_3NC(CH_2)_nCH_3]^+$, $n = 0$–17, have been synthesized and characterized. These complexes exhibit a unique intramolecular perturbation of their excited-state manifold by the normally passive alkyl chain. Intramolecular fold back, a strong function of chain length, alters the solvent environment around the excited portion of the molecule with a concomitant change in the state energies and decay paths. Molecular models, cyclodextrin binding studies, absorption and emission spectroscopy, excited-state lifetime measurements, and oxygen-quenching studies support this model. The alkyl chain can function as a molecular switch and invert the lowest excited states in the molecules at low temperature. Energy level diagrams are developed that explain both room-temperature and 77 K results.

Luminescent transition-metal complexes have been utilized as photosensitizers in such areas as solar energy conversion,[1] electron-transfer studies,[2] chemi- and electroluminescent systems,[3,4] binding dynamics of heterogeneous media,[5] and probes of macromolecular structure.[6] $Ru^{II}(L)_3^{2+}$ complexes (L = 2,2′-bipyridine, 1,10-phenanthroline, or substituted derivatives) have been the most frequently used probes in these applications due to strong visible absorption, high photochemical stability, efficient luminescence, and relatively long-lived metal to ligand charge-transfer (MLCT) excited states.[7]

Further, the emitting-state energies and excited-state redox properties of the sensitizers can be very sensitive to the nature of the metal, coordinating ligands, and solvent environment. Solvent and substituents have been used to control the relative positions of MLCT excited states and effectively "tune" their photophysical and photochemical properties.[8-10] Many of these sensitizers exhibit a wide variety of energetically accessible charge-transfer (CT), ligand-field (LF), and intraligand (IL) excited states. These excited states are of differing orbital parentage and, therefore, can have quite different excited-state characteristics. Since the photophysical properties of the metal complexes are determined predominantly by the lowest energy excited states,[11] it is important to understand thoroughly their excited-state energetics and dynamics in order to be able to design rationally new and more useful photosensitizers and probes.

For those sensitizers having lowest lying MLCT states, models are based predominantly on the photophysics and photochemistry of the $^*Ru(bpy)_3^{2+}$ (bpy = 2,2′-bipyridine) and related sensitizers, leading to a general picture of metal complex excited-state behavior. Recently, Os(II),[12] Ir(III),[13] Mo(0) and W(0),[14] and Re(I)[15,16] complexes have been studied with increasing interest. In some cases, these complexes exhibit even more desirable excited-state properties than the Ru(II) sensitizers.

An additional level of richness in the form of multiple luminescences has been observed for a number of transition-metal compounds with α-diimine ligands. As we will show, this allows the construction of systems that are highly sensitive to subtle changes in local environment. DeArmond and co-workers originally reported dual ligand-localized phosphorescences from heterochelated Rh^{3+} complexes.[17] Watts et al. observed multiple CT emissions from Ir^{3+} sensitizers.[13] Wrighton et al. have seen dual low-temperature emissions for a number of Re(I) carbonyl compounds.[16] McMillin and co-workers have reported mixed CT and IL emissions at 77 K from tetrahedral Cu(I) complexes.[18] Lees has reported dual MLCT emissions at room temperature for W(0) and Mo(0) carbonyl complexes.[19]

We have recently embarked on a detailed study of Re(I) photosensitizers of the form $[(bpy)Re(CO)_3NC(CH_2)_nCH_3]^+$, n

† Taken in part from: Reitz, G. A. M.S. Thesis, University of Virginia, 1987.

‡ Department of Chemistry, University of Virginia.

§ Department of Chemistry, James Madison University.

‖ Department of Physiology, University of Virginia.

(1) (a) Grätzel, M., Ed. *Energy Resources through Photochemistry and Catalysis*; Academic: New York, 1983. (b) Kalyanasundaram, K. *Coord. Chem. Rev.* **1982**, *46*, 159. (c) Balzani, V.; Bolletta, F.; Gandolfi, M. T.; Maestri, M. *Top. Curr. Chem.* **1978**, *75*, 1.

(2) (a) Creutz, C.; Sutin, N. *Proc. Natl. Acad. Sci. U.S.A.* **1975**, *72*, 2858. (b) Lin, C.; Sutin, N. *J. Phys. Chem.* **1976**, *80*, 97.

(3) (a) Tokel-Takvoryan, N. E.; Hemingway, R. E.; Bard, A. J. *J. Am. Chem. Soc.* **1973**, *95*, 6582. (b) Martin, J. E.; Hunt, E. J.; Adamson, A. W.; Gafney, H.; Halpern, J. *J. Am. Chem. Soc.* **1972**, *94*, 9283. (d) Lytle, F. E.; Hercules, D. M. *Photochem.* Photobiol. **1971**, *13*, 123.

(4) (a) Buttry, D. A.; Anson, F. A. *J. Am. Chem. Soc.* **1982**, *104*, 4824. (b) White, H. S.; Bard, A. J. *J. Am. Chem. Soc.* **1982**, *104*, 6891. (c) D. Bolletta, F.; Balzani, V. *J. Am. Chem. Soc.* **1982**, *104*, 4250. (d) Vogler, A.; El-Sayed, L.; Jones, R. G.; Namnath, J.; Adamson, A. W. *Inorg. Chim. Acta* **1981**, *53*, L35. (e) Kunkely, H.; Merz, A.; Vogler, A. *J. Am. Chem. Soc.* **1983**, *105*, 7241. (f) Luong, J. C.; Nadjo, L.; Wrighton, M. S. *J. Am. Chem. Soc.* **1978**, *100*, 5790.

(5) Kalyanasundaram, K. *Photochemistry in Microheterogeneous Systems*; Academic: New York, 1987.

(6) (a) Kumar, C. V.; Barton, J. K.; Turro, N. J. *J. Am. Chem. Soc.* **1985**, *107*, 5518. (b) Barton, J. K.; Lolis, E. *J. Am. Chem. Soc.* **1985**, *107*, 708. (c) Barton, J. K.; Danishefsky, A. T.; Goldberg, J. M. *J. Am. Chem. Soc.* **1984**, *106*, 2172. (d) Barton, J. K.; Basik, L. A.; Danishefsky, A.; Alexandrescu, A. *Proc. Natl. Acad. Sci. U.S.A.* **1984**, *81*, 1961.

(7) (a) Watts, R. J. *J. Chem. Educ.* **1983**, *60*, 834, and references therein. (b) Meyer, T. J. *Pure Appl. Chem.* **1986**, *58*, 1193, and references therein.

(8) (a) Watts, R. J.; Crosby, G. A. *J. Am. Chem. Soc.* **1971**, *93*, 3184. (b) Malouf, G.; Ford, P. C. *J. Am. Chem. Soc.* **1977**, *99*, 7213. (c) Ford, P. C. *Rev. Chem. Intermed.* **1979**, *2*, 267.

(9) (a) Pankuch, B. J.; Lackey, D. E.; Crosby, G. A. *J. Phys. Chem.* **1980**, *84*, 2061. (b) Pankuch, B. J.; Lackey, D. E.; Crosby, G. A. *J. Phys. Chem.* **1980**, *84*, 2068.

(10) (a) Sutin, N.; Creutz, C. In *Inorganic and Organometallic Chemistry*; Wrighton, M. S., Ed.; Advances in Chemistry Series 168; American Chemical Society: Washington DC, 1978; p 1. (b) Creutz, C.; Chou, M.; Netzel, t. L.; Okimura, M.; Sutin, N. *J. Am. Chem. Soc.* **1980**, *102*, 1309.

(11) (a) Kasha, M. *Discuss. Faraday Soc.* **1950**, *9*, 14. (b) Demas, J. N.; Crosby, G. A. *J. Am. Chem. Soc.* **1970**, *92*, 7262.

(12) (a) Kober, E. M.; Marshall, J. L.; Dressick, W. J.; Sullivan, B. P.; Caspar, J. V.; Meyer, T. J. *Inorg. Chem.* **1985**, *24*, 2755. (b) Caspar, J. V.; Kober, E. M.; Sullivan, B. P.; Meyer, T. J. *J. Am. Chem. Soc.* **1982**, *104*, 630. (e) Kober, E. M.; Sullivan, B. P.; Dressick, W. J.; Caspar, J. V.; Meyer, T. J. *J. Am. Chem.* Soc. **1980**, *102*, 1383.

(13) (a) Watts, R. J.; Brown, M. J.; Griffith, B. G.; Harrington, J. S. *J. Am. Chem. Soc.* **1975**, *97*, 6029 (b) Watts, R. J.; Griffith, B. G.; Harrington, J. S. *J. Am. Chem. Soc.* **1976**, *98*, 674.

(14) (a) Lees, A. J. *Chem. Rev.* **1987**, *87*, 711. (b) Connor, J. A.; Overton, C.; El Murr, N. *J. Organomet. Chem.* **1984**, *277*, 277. (c) Connor, J. A.; Overton, C. *Inorg. Chim.* Acta **1982**, *65*, L1. (d) Abrahamson, H. B.; Wrighton, M. S. *Inorg. Chem.* **1978** *17*, 3385. (e) Wrighton, M. *Chem. Rev.* **1972**, *74*, 401.

(15) (a) Caspar, J. V.; Sullivan, B. P.; Meyer, T. J. *Inorg. Chem.* **1984**, *23*, 2104. (b) Caspar, J. V.; Meyer, T. J. *J. Phys. Chem.* **1983**, *87*, 952.

(16) (a) Wrighton, M. S.; Morse, D. L. *J. Am. Chem. Soc.* **1974**, *96*, 998. (b) Luong, J. C.; Faltynak, R. H.; Wrighton, M. S. *J. Am. Chem. Soc.* **1979**, *101*, 1597. (c) Giordano, P. J.; Fredericks, S. M.; Wrighton, M. S.; Morse, D. L. *J. Am. Chem.* Soc. **1978**, *100*, 2257. (d) Fredericks, S. M.; Luong, J. C.; Wrighton, M. S. *J. Am. Chem. Soc.* **1979**, *101*, 7415. (e) Giordano, P. J.; Wrighton, M. S. *J. Am. Chem. Soc.* **1979**, *100*, 2888.

(17) Halper, W.; DeArmond, M. K. *J. Lumin.* **1972**, *5*, 225.

0002-7863/88/1510-5051$01.50/0

= 0–17. Our initial goal was to design cationic complexes that would anchor to cationic micelles. We predicted that for large enough n's the hydrophobic interactions would overcome electrostatic repulsions. Indeed, this worked well, and for $n \geq 5$, strong binding to cationic cetyltrimethylammonium bromide (CTAB) micelles was observed.

However, we also discovered the remarkable fact that, even in pure solvents, the electronically passive alkyl chain of the nitrile dramatically perturbed the emissions.[20] These changes were highly dependent on the alkyl chain length and resulted from an intramolecular foldback of the chain onto the bpy ligand. This fold back perturbed the solvent environment around the excited portion of the complex and altered the excited-state properties.

We report here on the detailed characterization of the excited-state properties of these Re(I) sensitizers. Our results show that the large n-dependent perturbations in excited-state properties arise from the proximity of two emitting excited states of different orbital parentage. This paper expands on our earlier results and elucidates the nature of the inter- and intramolecular interactions.

Experimental Section

Materials. $Re(CO)_5Cl$ (Pressure Chemical Co.) and bpy (GFS Chemical Co.) were used as received. Alkane nitriles, $CH_3(CH_2)_nCN$, were used as received from Aldrich Chemical Co. (n = 2, 7, 10), Chemical Procurement Laboratories, Inc. (n = 5, 9), and Pfalz and Bauer Chemical Co. (n = 13, 17). High-purity solvents (acetonitrile, methanol, dichloromethane, and toluene) were from Burdick-Jackson Laboratories or Fisher Scientific. Tetraethylammonium perchlorate (TEAP) (Eastman Kodak Co.) was recrystallized from water. All other inorganic salts and solvents were reagent grade. Neutral alumina (Fisher) was used for chromatography, α- and β-cyclodextrins (α-CD and β-CD) were from Sigma Chemical Co. Deionized water was redistilled from alkaline $KMnO_4$.

Syntheses. $(bpy)Re(CO)_3Cl$ was prepared as previously described.[15b,16a] Yields were quantitative, and the product was used without purification. The $[(bpy)Re(CO)_3NC(CH_2)_nCH_3](ClO_4)$ complexes were prepared by a modification of the literature preparation[16d] for the parent acetonitrile (n = 0) complex. Details of our preparation and microanalyses, which were satisfactory, are given in the supplementary material.

Equipment and Procedures. Absorption spectra were obtained with Cary 17 or Hewlett-Packard 8450A spectrophotometers.

Corrected emission spectra were obtained on a microcomputerized SLM Instruments 8000 single photon counting spectrofluorimeter. Spectra at 298 K were typically obtained with 350-nm excitation. Most spectra were collected from aerated solutions, as sample deoxygenation showed no effect on the emission band shape or position. Low-temperature (77 K) emissions were measured in 5:5:2 diethyl ether/isopentane/ethanol (EPA) glasses. Spectra were collected with excitation wavelengths of 275–410 nm.

All emission spectra were acquired at low micromolar concentrations. Given the good solvent characteristic of the media, ion-pairing effects should be minimal.

Cyclic voltammetry measurements were carried out on a BAS Model CV-1B potentiostat. Acetonitrile solutions of the Re(I) complexes (0.1 M TEAP) were deaerated by bubbling with N_2 in a single microelectrode cell compartment utilizing a glassy-carbon working electrode, a platinum-wire auxiliary electrode, and a saturated calomel or Ag/AgCl reference electrode. All potentials are reported vs SCE as $E_{1/2}$ values, where $E_{1/2} = 0.5(E_p^a + E_p^c)$, and E_p^a and E_p^c are the anodic and cathodic peak potentials, respectively. Calibration was vs ferrocene.

Excited-state lifetimes (τ's) were measured with a pulsed N_2 laser (337 nm) nanosecond decay time system and software.[21] Measurement at 298 K used a thermostated cell holder,[22] and 77 K measurements used a liquid-nitrogen Dewar.

Both single-exponential and nonexponential luminescence decay curves were observed. The single-exponential decays were fit by linear least squares to the semilogarithmic plots of intensity vs time.[21] The nonexponential decays were fit by nonlinear least squares[23,24] to a sum of two exponentials (eq 1) where $I(t)$ is the luminescent intensity at time t and

$$I(t) = K_s \exp(-t/\tau_s) + K_l \exp(-t/\tau_l) \quad (1)$$

the K's and τ's are the preexponential weighting factors and the excited-state lifetimes, respectively. The subscripts s and l refer to the short- and long-lived component, respectively. Within experimental error, all data were fit to single- or double-exponential decays over 2–5 half-lives using at least 250 points for single-exponential fits and 350 points for double-exponential fits. All reported single-exponential τ's are averages of at least five measurements (precision of ±3%) and are considered accurate to within ±10%.

Luminescence quantum yields, Φ_{em}, in deoxygenated acetonitrile were measured by the Parker–Rees method.[25,26] The quantum yield standard was deoxygenated aqueous $[Ru(bpy)_3]Cl_2$ (Φ_{em} = 0.042 at 25 °C),[27] and refractive index corrections were applied.[26]

Radiative (k_r) and nonradiative (k_{nr}) decay rate constants for the emissions were obtained from Φ_{em} and the observed lifetime, τ_{obsd} (eq 2 and 3). In eq 3 it is explicitly assumed that the emitting state is formed

$$\tau_{obsd} = (k_r + k_{nr})^{-1} \quad (2)$$

$$\Phi_{em} = k_r \tau_{obsd} \quad (3)$$

with unit efficiency. This condition is known to be fulfilled for the related MLCT excited states of Ru(II) and Os(II) α-diimine complex type sensitizers,[11b,28] and we assume the same is true for the Re(I) complexes.

To obtain sensitizer–cyclodextrin equilibrium binding constants, titration curves of τ vs [CD] were carried out as described earlier.[29] Measurements were made in either deaerated (nitrogen-purged) or oxygen-saturated (bubbled with pure oxygen) solutions. The $1/\tau$ vs [CD] data were fit by a simplex nonlinear least-squares routine.[24]

Stern–Volmer, K_{SV}'s, and bimolecular oxygen-quenching rate constants, k_q's, for sensitizers in pure solvent and aqueous CD solutions were obtained from the slopes of plots of τ_0/τ vs $[O_2]$ (eq 4). τ_0 and τ are

$$\tau_0/\tau = 1 + k_q\tau_0[O_2] = 1 + K_{SV}[O_2] \quad (4)$$

the photosensitizer lifetimes in the absence and presence of O_2, respectively. Literature values for the O_2 solubilities were used.[30] Oxygen solubility in the CD solutions was assumed to be the same as that for water.[29]

Results

Characterization. The parent complex with an acetonitrile ligand (n = 0) was previously determined by IR spectroscopy to be the facial isomer.[16d] Our n = 0 complex had an electronic spectrum and lifetime in good agreement with the published values.[16d] Since all of our Re(I) sensitizers contained the same coordination sphere and were synthesized by the same methods, we conclude that all are facial isomers.

The solid Re(I) complexes are thermally and photochemically relatively inert and are soluble in most organic solvents except alkanes. Their water solubility decreases with increasing n; we could not prepare aqueous solutions of the n = 17 complex. In solution, the longer alkyl chain sensitizers are stable for a few days, but noticeable changes in the luminescence properties of the shorter alkyl chain complexes ($n \leq 7$) occur if the solution is left standing for more than 1 or 2 days. This behavior is more pronounced in polar solvents (e.g. H_2O, methanol, and acetonitrile) and is independent of exposure to room lights. Similar Re(I) sensitizers have previously been photoreduced through electron transfer from

(18) (a) Buckner, M. T.; Matthews, T. G.; Lytle, F. E.; McMillin, D. R. *J. Am. Chem. Soc.* **1979**, *101*, 5846. (b) Rader, R. A.; McMillin, D. R.; Buckner, M. T.; Matthews, T. G.; Casadonte, D. J.; Lengel, R. K.; Whittaker, S. B.; Darmon, L. M.; Lytle, F. E. *J. Am. Chem. Soc.* **1981**, *103*, 5906. (c) Casadonte, D. J. *jr.*; McMillin, D. R. *J. Am. Chem. Soc.* **1987**, *109*, 331.
(19) (a) Manuta, D. M.; Lees, A. J. *Inorg. Chem.* **1983**, *22*, 572. (b) Manuta, D. M.; Lees, A. J. *Inorg. Chem.* **1986**, *25*, 1354.
(20) Reitz, G. A.; Dressick, W. J.; Demas, J. N.; DeGraff, B. A. *J. Am. Chem. Soc.* **1986**, *108*, 5344.
(21) (a) Turley, T. J. MS Thesis, University of Virginia, 1980. (b) Turley, T. J.; Demas, J. N.; Demas, D. J. *Anal. Chim. Acta*, in press.
(22) Buell, S. L.; Demas, J. N. *Anal. Chem.* **1982**, *54*, 1214.
(23) Marquardt, D. W. *J. Soc. Ind. Appl. Math.* **1963**, *11*, 431.
(24) (a) Daniels, R. W. *An Introduction to Numerical Methods and Optimization Techniques*; North-Holland: New York, 1978. (b) Demas, J. N. *Excited State Lifetime Measurements*; Academic: New York, 1983.
(25) Parker, C. A.; Rees, W. T. *Analyst (London)* **1962**, *87*, 83.
(26) Demas, J. N.; Crosby, G. A. *J. Phys. Chem.* **1971**, *75*, 991.
(27) Van Houten, J.; Watts, R. J. *J. Am. Chem. Soc.* **1976**, *98*, 4853.
(28) (a) Demas, J. N.; Taylor, D. G. *Inorg. Chem.* **1979**, *18*, 3177. (b) Taylor, D. G.; Demas, J. N. *J. Chem. Phys.* **1979**, *71*, 1032.
(29) Cline, J. I., III; Dressick, W. J.; Demas, J. N.; DeGraff, B. A. *J. Phys. Chem.* **1985**, *89*, 94.
(30) Battino, R., Ed. *IUPAC Solubility Data Series*; Pergamon: Great Britain, 1981; Vol. 7.

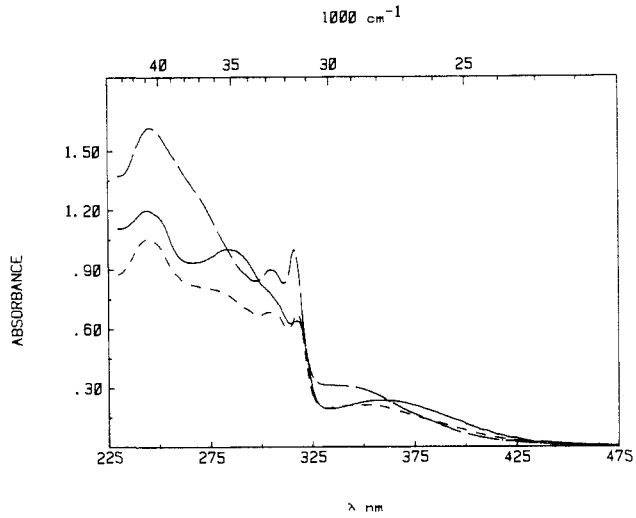

Figure 1. Room-temperature absorption spectra of $Re(byp)(CO)_3NC(CH_2)_nCH_3^+$ in CH_2Cl_2 (1-cm cells): $n = 0$ (—), 71 μM; $n = 5$ (---), 58 μM; $n = 13$ (-·-), 75 μM.

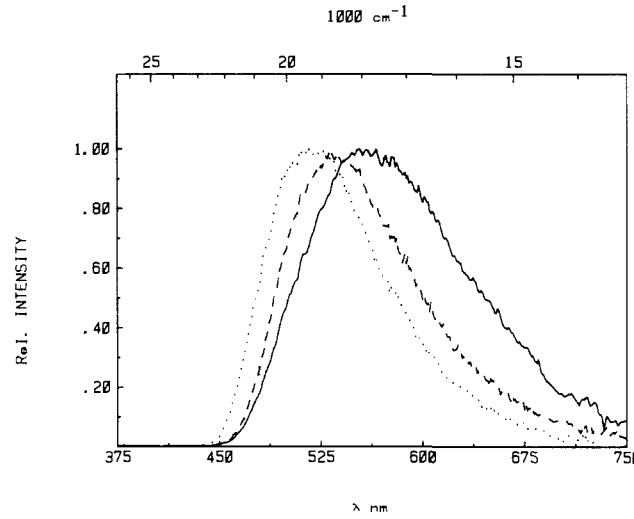

Figure 2. Room-temperature luminescence of $Re(bpy)(CO)_3NC(CH_2)_nCH_3^+$ in CH_2Cl_2: $n = 0$ (—); $n = 5$ (---); $n = 13$ (···).

some reducing agent, followed by efficient ligand substitution on the Re(0) and reoxidation to give new Re(I) products.[31] At this point, however, we are unable to come to any conclusions about our decomposition products.

As we will show, the $n = 0$ complex differs significantly in many of its photophysical properties compared to the $n = 2$ complex. Thus, there appears to be a large difference in the electronic inductive effect of a CH_3, vs a CH_2 on the excited states. We find that the $n = 2$ complex is a much better base-line molecule than the $n = 0$ one for comparison with the longer alkyl chain species.

Absorption Spectra. Absorption spectra of three representative Re(I) sensitizers at room temperature in CH_2Cl_2 are shown in Figure 1. The $n = 2$ complex has a spectrum that is indistinguishable from that of the $n = 5$ complex. Both, however, are clearly different from the $n = 0$ complex; this supports our earlier statement that the $n = 0$ complex makes a poor reference molecule.

The spectral band maxima and molar extinction coefficients for a number of the complexes are summarized in the supplementary material. In general, all of the Re(I) probes exhibit relatively intense low-energy absorptions centered in the 320–360-nm range. These low-energy bands fall substantially to the blue of the first absorptions in the parent $(bpy)Re(CO)_3Cl$ species.[16a,32] Very intense ($\epsilon \approx (1.5\text{–}2.5) \times 10^4$ M^{-1} cm^{-1}) higher energy absorption bands are also observed.

The spectral maxima of the low-energy absorption band around 350 nm and the more intense higher energy absorption at about 275 nm depends dramatically on the length of the alkyl chain (Figure 1). For both absorptions, the band maxima blue-shift by at least 2500 cm^{-1} with increasing n. This spectral shift is not unique to CH_2Cl_2 solutions but is present in all solvents examined (see supplementary material).

Luminescence Data. Room-temperature emission spectra for three representative Re(I) probes in CH_2Cl_2 are shown in Figure 2. As with the absorption spectra, the emission spectra of the $n = 2$ and 5 complexes are the same but differ significantly from that of the $n = 0$ complex. All spectra were similarly broad and unstructured in a number of organic solvents of varying polarity. The Re(I) emissions are sensitive to n (Figure 2) and to the solvent medium. Emission maxima and bandwidth as a function of solvent and n are summarized in the supplementary material. All the bandwidths are about the same in a given solvent except for the $n = 0$ complex where the bandwidth is appreciably broader than those for any of the other complexes.

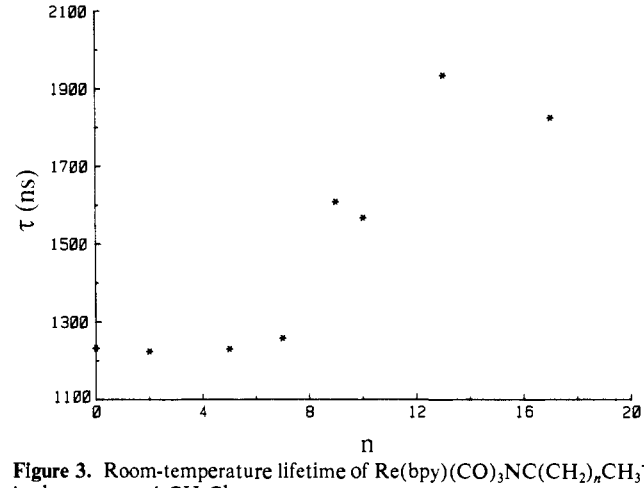

Figure 3. Room-temperature lifetime of $Re(bpy)(CO)_3NC(CH_2)_nCH_3^+$ in deoxygenated CH_2Cl_2 vs n.

Table I. Luminescent Quantum Yields and Radiative and Nonradiative Constants for $[(bpy)Re(CO)_3NC(CH_2)_nCH_3]^+$ in Acetonitrile (298 K)

n	Φ_{em}	$k_r \times 10^5$, s^{-1}	$k_{nr} \times 10^6$, s^{-1}
0	0.015	0.28	1.76
2	0.069	1.23	1.65
5	0.084	1.49	1.62
7	0.097	1.63	1.51
9	0.137	1.65	1.04
10	0.154	1.91	1.05
13	0.190	1.81	0.77
17	0.138	1.38	0.87

Luminescent lifetimes at 298 K for the $Re^I(bpy)$ species in deoxygenated CH_2Cl_2 as a function of n are plotted in Figure 3. As noted previously for other solvents,[20] τ is virtually independent of chain length for small n's. An abrupt increase in τ is seen over the range $7 \leq n \leq 13$, followed by an essentially constant τ for long chain lengths. The Re(I) series demonstrates this type of behavior with every solvent studied although the initial and final plateau lifetimes vary with solvent.

The k_q's for oxygen quenching in CH_2Cl_2, where we were able to make measurements over the entire range of n, show behavior similar to the τ vs n data. k_q was constant at 3×10^9 M^{-1} s^{-1} for $n = 2$, 5, and 7 and decreased to a constant value of about 2×10^9 M^{-1} s^{-1} for $n = 13$ and 17. Relative luminescence quantum yields, Φ_{em}, at 298 K in acetonitrile are reported in Table I along with k_r and k_{nr}.

Low-temperature emission spectra for several different complexes ($n = 5$, 7, 10, and 13) are shown in Figure 4 for both

(31) (a) Summers, D. P.; Luong, J. C.; Wrighton, M. S. *J. Am. Chem. Soc.* **1981**, *103*, 5238. (b) Fredericks, S. M.; Wrighton, M. S. *J. Am. Chem. Soc.* **1980**, *102*, 6168.

(32) Reitz, G. A., unpublished results.

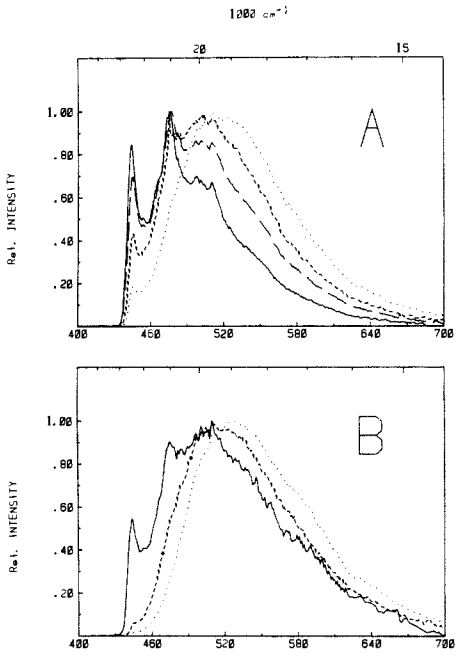

Figure 4. Low-temperature total luminescence spectra of Re(bpy)-$(CO)_3NC(CH_2)_nCH_3^+$ in EPA glass at 77 K: n = 5 (···); n = 7 (- - -); n = 10 (– –); n = 13 (—). A is for 350-nm excitation. B is for 410-nm excitation.

Table II. Lifetime Decay Parameters for $[bpyRe(CO)_3NC(CH_2)_nCH_3]^+$ Sensitizers in EPA at 77 K

n	λ_{em}, nm	K_l/K_s	τ_s, μs	τ_l, μs	f_l
5	442	0.64	5.5	18.0	0.39
	520	0.49	4.5	15.9	0.33
9	442	1.33	7.7	20.3	0.57
	520	1.10	5.7	24.6	0.52
13	442	2.6	8.1	21.2	0.72
	520	1.8	7.0	19.7	0.64

Table III. Properties of $[bpyRe(CO)_3NC(CH_2)_nCH_3]^+$–Cyclodextrin Inclusion Complexes

	K_{CD}, M^{-1}	
n	β-CD	α-CD
5	no effect	no effect
9	6000	150
13	10800	no effect
	$k_q(O_2) \times 10^{-9}$, M^{-1} s^{-1} ($K_{SV}(O_2)$, M^{-1})	
n = 9	β-CD	α-CD
free	2.08 (1220)	2.01 (1190)
CD bound	1.56 (750)	1.45 (1000)

350-nm (A) and 410-nm (B) excitation. The n = 7 spectrum was omitted for the 410-nm excitation because it is virtually identical with that of the n = 5 complex. The emission spectra were the same for 275-, 320-, and 350-nm excitation.

Table II shows the results of resolving the low-temperature decay curves for the n = 5, 9, and 13 complexes. Emission was monitored at either 442 or 520 nm.

Figures 5 and 6 show β-cyclodextrin titration curves for the n = 9 and 13 complexes. For the n = 9 complex we show the curves for both deaerated (A) and oxygen-bubbled (B) solutions along with the best single-component fits. The same binding constant was used for both the oxygenated and deaerated theoretical curves. The best double CD binding fit is also shown for the n = 13 complex. The results for the single-component binding constants and oxygen-quenching constants are given in Table III.

Electrochemical Results. The $E_{1/2}$ values for the n = 5, 7, 9, and 13 complexes in acetonitrile showed that both the oxidation and the first reduction waves were reversible on the electrochemical

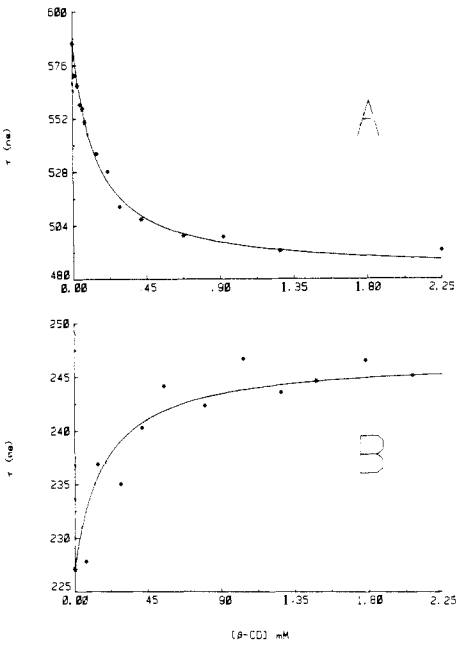

Figure 5. Lifetime titration of $Re(bpy)(CO)_3NC(CH_2)_9CH_3^+$ with β-CD in deoxygenated (A) or oxygen-bubbled (B) water. Additional points to 10 mM [CD] are omitted to show more clearly the changing portion of the curve. The solid lines are the best fits using the K_{CD} of Table III.

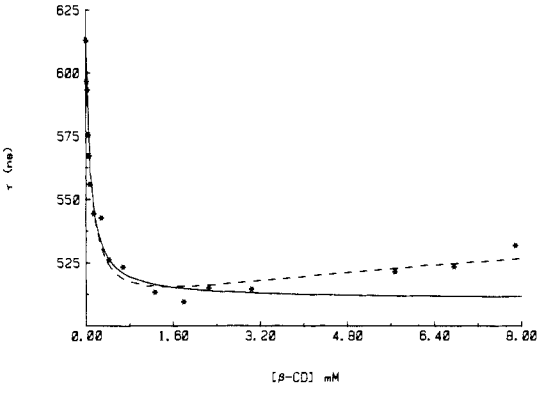

Figure 6. Lifetime titration of $Re(bpy)(CO)_3NC(CH_2)_{13}CH_3^+$ with β-CD in deoxygenated water. The solid line is the best fit ([CD] < 2 mM) using a single-CD binding and the K_{CD} of Table III. The dashed line is the best fit using a one- and two-CD binding model (Figures 8 and 9) with K_{CD} = 9300 M^{-1} and K_{2CD} = 100 M^{-1}. In the fitting, the lifetime of the $Re(CD)_2$ complex was limited to less than τ for the free sensitizer.

time scale. The $Re^{II/I}$ oxidation couple occurred around +1.85 V, irrespective of alkyl chain length. The first reduction wave occurred around −1.25 V, and this wave is followed by one or more irreversible waves. The reversible wave becomes slightly more cathodic with increasing n (0.05 V). There are no large shifts in potentials mirroring those seen in emission and absorption energies and τ's as a function of n.

Discussion

Any model for our Re(I) complexes must account for the changes in absorption and emission properties with alkyl chain length, solvent, and temperature, the CD effects, and the quenching effects. We will describe an expanded version of our earlier model[20] that accounts for all of these properties.

In our model we ascribe the changes in properties with increasing n as arising from an intramolecular fold back of the alkyl chain onto the face of the bipyridine ligand. This displaces the solvent and changes the local solvent environment around the excited portion of the molecule, which results in changes in the state energies and decay rates. See Figure 7.

In particular, this fold-back model accounts for the remarkable dependence of τ vs chain length (Figure 3 for CH_2Cl_2 and ref 20).

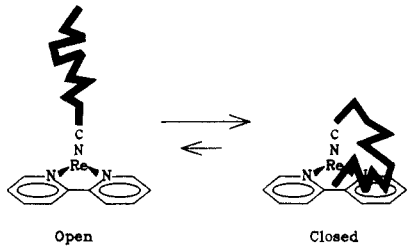

Figure 7. Simple intramolecular fold-back model.

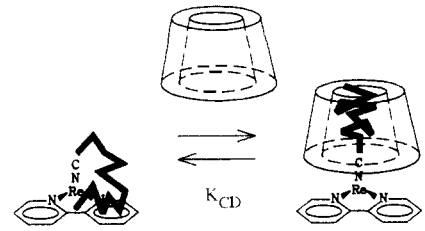

Figure 8. Model for the interaction of one CD with alkyl chain of $Re(bpy)(CO)_3NC(CH_2)_nCH_3^+$.

For $n \leq 5$, τ is essentially independent of n. For n in the range 7–13, τ increases rapidly. For $n \geq 13$, τ again plateaus at a value substantially higher than that for the earlier plateau.

Molecular models support this fold-back picture. For n less than 6, the alkyl chain is incapable of folding back onto the bpy ring and, thus, cannot affect the local solvent environment and the decay processes. For $n \geq 13$ the chain can virtually cover the upper face of the bpy. Even for $n = 17$, however, the chain cannot simultaneously cover the front, wrap around the bpy, and also shield the opposite face. For n between 6 and 13, however, the degree of coverage of the one bpy face can be highly dependent on n and the luminescence decay properties are likewise sensitive to n. See the photographs of ref 20.

Such an intramolecular fold back has also been observed by NMR in copper and zinc 1,10-phenanthroline (phen) complexes coordinated with alkanecarboxylic acids.[33] With increasing n, the alkyl chain spent more time folded over the exposed phen face; that is, the equilibrium constant for formation of the closed form in which the alkyl chain is folded over the phen face increases with n. Even for relatively long chains, however, the percentage of folded or closed form did not greatly exceed 40%.

Our current results support and expand on this picture of an intramolecular fold back, which modifies the excited-state properties. We will assign the absorption and emission spectra, discuss the solvent effects, and correlate them to the intramolecular fold-back interactions. We then explain the effect of oxygen quenching, cyclodextrin binding, and the surprisingly high sensitivity of the luminescence properties to n.

Absorption Spectra. The absorption bands at about 245, 305, and 318 nm can be clearly ascribed to ligand-localized $\pi-\pi^*$ transitions. This assignment is based on the striking similarity in energy, extinction coefficient, and band shape to the transitions observed in protonated bpy[34] and aqueous $Rh(bpy)_3^{3+}$, $Zn(bpy)^{2+}$, and $Zn(bpy)_3^{2+}$ where CT states are minimal or absent.[35] For example, $Zn(bpy)^{2+}$ has ligand bands at 244, 295, and 306 nm, and $Rh(bpy)_3^{2+}$ has bands at 242, 306, and 319 nm.

The intense transitions at about 275 and 330–360 nm are clearly different from the ligand transitions. We assign these bands to CT transitions. These bands do not occur in the spectra of the uncoordinated bpy ligand or the $Re(CO)_5Cl$ starting material. Further, unlike the $\pi-\pi^*$ transitions that are largely insensitive to solvent or variation in n, these transitions are highly sensitive to changes in local environment as affected by changes in the solvent or by the chain length of the alkyl substituent. The transitions are too strong and too solvent-sensitive to be ligand-field transitions. Thus, they are clearly CT in nature.

We assign the low-energy band as a MLCT transition as it is too low in energy to be metal to carbonyl. The low-energy band in the analogous $n = 0$ phen complex has been previously assigned to an MLCT absorption.[16d]

We also assign the higher energy 275-nm transition to a metal to bpy CT state. While not definitive, this assignment is based on the striking similarity of the solvent and n sensitivity of the 275-nm band and the lower energy metal to bpy CT transition (supplementary material and unpublished results). In particular, the state energies (λ_{max}) shift in the same direction and by about the same amount for both CT states in response to changes in n and solvent, although, for the shorter wavelength bands, it is not possible to resolve peak positions because of overlap with the 245-nm band. Further, if the 275-nm transitions were metal to CO CT bands, we would expect the intramolecular fold back to the bpy ring to affect these bands in a different fashion than the metal to bpy CT transitions, which is not observed. Finally, analogous pairs of MLCT transitions are well-known in the visible and near-UV spectra of W(0) and Mo(0) α-diimine systems, and both bands show significant and similar shifts in response to changes in the solvent.[36,37]

The important feature of the n dependence of the CT state absorptions (supplementary material) is the following: In a single solvent, the state energy does not change as n changes from 2 to 5, but λ_{max} decreases with n from $n = 5$ to 13. It appears that λ_{max} may be the same for $n = 13$ and 17, but the strong blue shift with increasing n makes it difficult to resolve these bands in the presence of the more intense $\pi-\pi^*$ transitions. This behavior is identical with that observed for the n dependence of τ.

A blue shift on decreasing environmental polarity is well-known for the emissions and absorptions of charge-transfer transitions in organic environmental polarity probes.[38] This further supports our original interpretation of a decreasingly polar environment around the excited state as n increases. We stress that the solvent effects are complicated, and, with the limited number of solvents studied, we can draw no conclusions about the microscopic details of solvent–complex interactions.

Oxygen-Quenching Constants. The variations in k_q's vs n in CH_2Cl_2 further support the fold-back phenomena. If fold back of the hydrocarbon tail onto the bpy face occurs, we would expect shielding of the emitting level from a solvent-borne quencher and a reduction of k_q with n (supplementary material). There is roughly a 30% reduction in k_q on going from the short- to long-chain complexes in CH_2Cl_2. The plateaus and breaks in the k_q vs n curves follow those seen in the lifetime data.

We attribute the reduction in k_q with increasing n to intramolecular shielding. The small effect is not surprising, since at most one face of the bpy can be covered by the alkyl group, and shielding is, thus, only partial. Also, oxygen is a small, very mobile quencher with a high solubility in hydrocarbons,[30] which may further reduce the effectiveness of shielding by the tail. However, there is no doubt that there is some form of chain length dependent intramolecular shielding in CH_2Cl_2. Since k_q shows no discernible change with n in acetonitrile, it is clear that specific, and as yet not understood, solvent effects can also be important.

Cyclodextrin Binding. If the intramolecular fold-back model is correct, anything that alters the interaction of the hydrocarbon

(33) (a) Sigel, H.; Malini-Balakrishnan, R.; Haring, U. K. *J. Am. Chem. Soc.* **1985**, *107*, 5137. (b) Malini-Balakrishnan, R.; Scheller, K. H.; Haring, U. K.; Tribolet, R.; Sigel, H. *Inorg. Chem.* **1985**, *24*, 2067. (c) Sigel, H.; Fischer, B. E.; Farkas, E. *Inorg. Chem.* **1983**, *22*, 925. (d) Sigel, H. *Angew. Chem., Int. Ed. Engl.* **1982**, *6*, 389.

(34) Gondo, Y.; Kanda, Y. *Bull. Chem. Soc. Jpn.* **1965**, *41*, 39.

(35) (a) Carstens, D. W. H. Ph.D. Dissertation, University of New Mexico, 1968. (b) Yamasaki, K. *Bull. Chem. Soc. Jpn.* **1937**, *12*, 390. (c) Sone, K.; Krumholz, P.; Stammreich, H. *J. Am. Chem. Soc.* **1955**, *77*, 777.

(36) (a) Dodsworth, E. S.; Lever, A. B. P.; Eryavac, G.; Crutchley, R. J. *Inorg. Chem.* **1985**, *24*, 1906. (b) Daamen, H.; Oskam, A.; Stufkens, D. J.; Waaijers, H. *Inorg. Chim. Acta* **1979**, *34*, 253.

(37) (a) Balk, R. W.; Stufkens, D. J.; Oskam, A. *Inorg. Chim. Acta* **1979**, *34*, 267. (b) Balk, R. W.; Stufkens, D. J.; Oskam, A. *Inorg. Chim. Acta* **1978**, *28*, 133. (c) Staal, L. H.; Stufkens, D. J.; Oskam, A. *Inorg. Chim.* Acta **1978**, *26*, 255.

(38) Lakowicz, J. R. *Principles of Fluorescence Spectroscopy*; Plenum: New York, 1983.

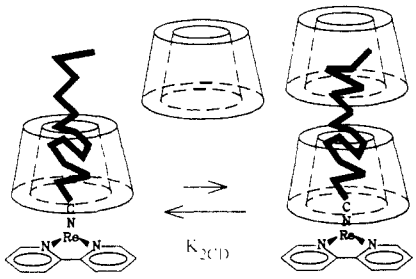

Figure 9. Model for the interaction of a second CD with extended alkyl chain of $Re(bpy)(CO)_3NC(CH_2)_{13}CH_3^+$.

tail with the excited portion of the molecule should affect the excited-state decay processes. We have shown that β-cyclodextrin (β-CD) binds with phenyl substituents on bpy and phen complexes of Ru(II) by formation of inclusion complexes.[29] Judging from the water solubility of our alkyl Re(I) complexes, we reasoned that the alkyl chains should be as hydrophobic as the phenyl groups and should also form inclusion complexes with CD's. This supposition was borne out.

As judged by τ's, there was no evidence of CD binding for $n = 0$ and 5. Bound CD is not electronically passive and would alter the excited-state lifetime if it were slipped over a short alkyl chain.[29] Thus, α- and β-CD do not interact with the $Re(bpy)(CO)_3$– portion of the molecule or with very short alkyl chains. This result is consistent with our earlier findings that β-CD does not bind to Ru(II) complexes that contain only bpy, phen, Me_2-phen, or Me_4-phen ligands.[29] For the $n = 9$ complex, however, Figure 5 clearly shows that τ varies with [β-CD] and the shapes of the titration curves are highly dependent on the oxygen concentration. We attribute these changes to binding of CD to the alkyl chain.

Figure 8 shows our proposed model. CD pulls the alkyl chain away from the bpy, alters the environment around the bpy, and changes the excited-state decay paths.

In the absence of oxygen, τ decreases with increasing [CD]. We attribute this to removal of the alkyl group from the bpy, which exposes it to more solvent or to the OH groups of the CD face. In either case enhanced deactivation of the excited state will occur, and τ will shorten.

In the presence of oxygen the lifetime increases with increasing [CD]. We attribute this to an increased shielding of the excited state by the bulky CD vs the more penetrable alkyl group.

Our results show that CD binding does not result in total replacement of the alkyl chain on the upper bpy face by water. For the unshielded $n = 5$ complex in pure deaerated water, τ is 250 ns. If CD binding to the $n = 9$ complex fully exposes the upper bpy face to water, we would expect τ to fall to this value, but τ is about a factor of 2 longer than for a fully water-exposed excited state. Thus, in the inclusion complex, CD shields the excited state at least partially from water exposure.

The oxygenated results also show that CD does not completely expose the bpy to water. If full exposure occurred, τ of the CD inclusion complex in the oxygenated solvent should fall to the 175-ns lifetime of the $n = 5$ complex. But the lifetime of the inclusion complex actually increases. Thus, we conclude that CD binding pulls the alkyl chain away from the bpy face. In the process the CD must sit over the nitrile and block the free entry of water or oxygen to the one face of the bpy.

Fitting the $1/\tau$ vs [CD] data allowed us to estimate K_{CD} and the τ of the bound form. Table III summarizes our K_{CD} data for α- and β-CD. The model of Figure 9 quantitatively fit all the data except for the $n = 13$ case (Figure 6). For $n = 13$, the titration curve is distinctly biphasic, showing first a large and rapid decrease in τ and then a slow increase. This behavior was very reproducible and was not seen with the shorter n's.

For the β-CD there is a large increase in K_{CD} with increasing n. The driving force for formation of CD complexes is displacement of water from the hydrophobic core of the CD by the hydrophobic guest.[39] We attribute the increasing K_{CD} with n to the larger amount of water that can be displaced by the longer alkyl chain; we assume that the alkyl chain will pack into the CD cavity. This is consistent with the much smaller binding constant for the $n = 9$ complex of α-CD vs β-CD. The α-CD cavity is much smaller, and the driving force is limited by the smaller number of water molecules that can be displaced.

It seems unlikely that the $n = 9$ complex binds to α-CD while the $n = 13$ does not. However, our monitoring method detects only changes in the environment around the emitting portion of the molecule. Molecule models show that α-CD can only cap the end of the alkyl chain and cannot efficiently slide down over the chain. For the α-CD bound to the $n = 13$ complex, the α-CD sits at the end of the chain that overlays the bpy, but it cannot pull the chain off of the bpy face. Thus, it exerts only minor perturbations on the excited portion of the complex. We conclude that binding is occurring but that our monitoring method is insensitive to inclusion complex formation.

We suggest that the biphasic behavior for the $n = 13$ complex with β-CD is because the chain is long enough to completely fill the CD cavity and still have some of the chain penetrate completely through the CD and emerge on the other side. We believe that the appearance of a second binding is due to interaction of the protruding portion of the alkyl chain with a second CD. See Figure 9. We refer to this as shish-kabob binding. We can quantitatively model the titration curve by including binding of the second CD (see the fit of Figure 6), although the fit parameters have very large uncertainties. It is clear, however, that K_{2CD} is at least 1–2 orders of magnitude smaller than K_{CD}. This is reasonable since the shorter free length of alkyl chain can displace less water from the second CD molecule.

Further support of shish-kabob binding comes from earlier kinetic studies. Dual binding of a surfactant molecule to two α-CD's has been observed.[40] However, both ends of the surfactant alkyl chain were free, and one CD could slip over each end. In our case, one end of the CD is blocked by the metal portion of the molecule, and both CD's must interact from only one end.

Room-Temperature Emission Spectra. The room-temperature emission spectra are broad and structureless. The emission maxima and band shapes for the different complexes are independent of excitation wavelength (275–400 nm). The dominant emission is a long-lived exponential decay, but there is some evidence for a weak, short-lived (<50-ns) component with short alkyl chain length complexes, especially with $n \leq 7$. This result is consistent with a dominant emission from a single low-lying excited state.

While the lowest bpy $^3(\pi-\pi^*)$ state falls at an energy that could give rise to the observed room-temperature emissions, several lines of reasoning argue against this assignment. The emission maxima track the observed shifts in the lowest energy CT absorption bands with variation in n. Several of the emissions seem much too low in energy to arise from a ligand state. Further, the room-temperature intrinsic excited-state lifetimes (vide infra) are consistent with an emission arising from a predominantly MLCT state. A similar assignment has been made for the emissions of other Re(I) α-diimine complexes.[16] As we will show, however, the excited-state manifold of this system is much more complicated, especially at low temperatures, than this simple analysis might suggest.

Having discussed the qualitative features of the fold back of Figure 7, we turn now to the rather remarkable impact of this effect on the excited-state energies. In addition to examining the quantitative consequences of this effect, we present an excited-state model that correctly interprets all our data.

Room-Temperature Rate Constants. Table I shows the radiative and radiationless decay rate constants at room temperature. The

(39) (a) Bender, M. L.; Komiyama, M. *React. Struct.: Concepts Org. Chem.* **1978**, *6*. (b) Saenger, W. In *Inclusion Compounds*; Atwood, J. L., Davies, J. E. D., MacNicol, D. D., Eds.; Academic: London, 1984; Vol. 2. (c) Szejtli, J. In *Inclusion Compounds*; Atwood, J. L., Davies, J. E. D., MacNicol, D. D., Eds.; Academic: London, 1984; Vol. 3, p 332. (d) Bergeron, R. J. In *Inclusion Compounds*; Atwood, J. L., Davies, J. E. D., MacNicol, D. D., Eds.; Academic: London, 1984; Vol. 3.

(40) Hersey, A.; Robinson, B. H.; Kelly, H. C. *J. Chem. Soc., Faraday Trans 1* **1986**, *82*, 1271.

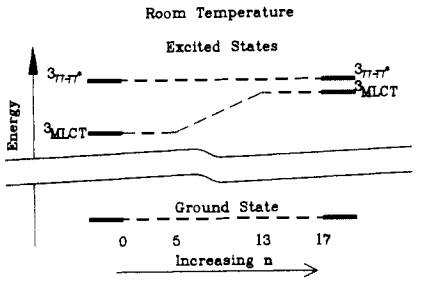

Figure 10. Room-temperature excited-state diagram for the lowest states of $Re(bpy)(CO)_3NC(CH_2)_nCH_3^+$ as a function of n.

luminescence quantum yields are remarkably high for room-temperature solutions of species with such long excited-state lifetimes. The changes in yield with n are largely a consequence of changes in k_{nr}'s. The k_r's are largely independent of n. As before, the $n = 0$ case is not representative and is excluded from further discussion.

The radiative lifetimes, $1/k_r$, are about 6 μs and are relatively constant with n ($n > 0$). This intrinsic lifetime is comparable to the 10–20-μs intrinsic τ's for CT emissions of similar Ru(II) complexes with α-diimine ligands.[11b,41] The shorter intrinsic lifetime is attributable to the higher atomic number of Re vs Ru with a concomitant increase in the degree of spin–orbit coupling and a shortening of the intrinsic lifetime. Similar results have been seen for Os vs Ru complexes.[11b,42]

We conclude that the room-temperature emission of the complexes is predominantly MLCT in character. There does appear to be a small decrease in the intrinsic lifetime with n, but this falls within the range observed for environmental effects on k_r. Since we attribute the changes in lifetime and emission spectra to a change in environment around the excited state, these small changes in k_r are not surprising.

The major cause of the changes in lifetime and quantum yield is the change in k_{nr}. Displacement of the solvent from around the excited state by the alkyl chain reduces k_{nr}. This is probably due to an energy gap law effect,[15b] since a plot of ln k_{nr} vs emission energy is linear if the $n = 0$ complex is excluded.

Figure 10 shows an energy level diagram that accounts for the room-temperature results. The MLCT state is below the ligand-localized $^3(\pi-\pi^*)$ state for small n's. For increasing chain length in the 5–13 range, the MLCT state is pushed to higher energy. For very long chains the MLCT state energy effectively becomes constant, but even for the longest chain complex the MLCT state appears to be the lowest energy excited state; the constancy of k_r supports the common orbital parentage of the emitting state with n.

For convenience of labeling we use singlet and triplet notations for the CT states. In fact, spin–orbit coupling is very large in the CT states, and S is not a good quantum number. The CT states are best described as spin–orbit states. Indeed, the emitting CT state of $Ru(bpy)_3^{2+}$ can function as both a very efficient singlet and triplet sensitizer.[43] In the current context, we use a singlet notation to denote an allowed transition with a high extinction coefficient and a triplet notation for the less strongly absorbing transition that gives rise to the emission.

We turn now to the room-temperature solution equilibria. For a rapid interconversion of the open and closed forms (Figure 7), the observed lifetime is given by eq 5 where f_{open} and f_{closed} are

$$1/\tau_{obsd} = f_{open}(1/\tau_{open}) + f_{closed}(1/\tau_{closed}) \quad (5a)$$

$$f_{open} + f_{closed} = 1 \quad (5b)$$

the fraction of the opened and closed forms in solution and the same notation is used for the excited-state lifetimes. The ratio $\tau_{obsd}(n = 2)/\tau_{obsd}(n = 13)$ varies from 0.43 (methanol) to 0.63 (CH_2Cl_2 and pyridine) where the $n = 2$ must be fully open. We can rearrange eq 5 to solve for f_{open}. If we assume that τ_{open} is independent of n (equal to $\tau_{obsd}(n = 2)$) and τ_{closed} cannot be negative, then f_{open} must fall in the range of zero to this ratio (0.43–0.63 depending on solvent).

In fact, the sigmoidal lifetime curve suggests that the closed form dominates for larger n's. In spite of the rapid rise in lifetime from $n = 7$ to 13, there is no appreciable change between $n = 13$ and 17. Further, the fractional change in τ matches closely the maximum fractional coverage of the bpy face for each n value. These results are most easily explained if the closed form is always the dominant conformer. Our conclusion is different than that drawn for Sigel's Cu and Zn systems[33] where, even for the longer chains, fold back never approached 50%. Further, they were able to disrupt fold back by using less polar solvents, an effect that does not appear to occur in our systems. Since there is no obvious difference chemically, we suggest that there is a large difference in the fold-back equilibrium constant on going from the ground to the excited state. This is not unreasonable since the excited state has an unpaired electron in the π-antibonding orbital of the bpy, which can greatly affect its polarizability and other interactions. While we cannot exclude a difference caused by the different geometries of the Cu and Zn systems vs the Re(I) complexes, molecular models suggest that there are no obvious barriers to fold back in Sigel's systems, and we would expect similar behavior.

There are suggestions of preferred microstructures for some n's. For example, we find a consistent glitch in the τ vs n plots at the $n = 9$ and 10 values. There is a similar effect in the emission spectra λ_{max} vs n. While near our experimental errors, these effects are so consistent as to lead us to believe that there is something unusual in either the stability or the decay paths around the $n = 9$ and 10 structures, and, thus, the series does not follow a simple monotonic progression with n.

For the very long $n = 17$ case there may also be a deviation from our pristine model. For several solvents (e.g. acetonitrile, CH_2Cl_2, and toluene), τ for the $n = 17$ complex dips somewhat below that of the $n = 13$ complex. The $n = 17$ complex could have another favorable conformation besides direct fold back onto the nearest bpy face. For example, rather than coiling onto the near face of the bpy, the chain may extend over the front face, wrap around the bpy, and partially cover the back face. This configuration does not give complete coverage of the far face and leaves the front bpy face more exposed to the solvent than in the more direct foldback model but still gives considerable solvent shielding. The greater solvent exposure of this form would give a reduction in τ relative to full front face coverage.

In spite of the large effect of n on absorption and emission properties, there is a very minimal effect on the electrochemistry. We attribute this to the relatively small overall shielding of the complex and the dynamic nature of the fold back. As the complex approaches the electrode, open structures are rapidly produced and can be freely sampled by the electrode.

Low-Temperature Emission Spectra. The emissions at 77 K (Figure 4) exhibit a spectacular change in character as n increases from $n = 0$–5 to $n = 13$ and 17, particularly for the 350-nm excitation. The broad structureless emission for $n < 7$ acquires increasing amounts of a highly structured component as n increases. By $n = 13$ the emission is dominated by the structured component, although there is still a suggestion of the broad component. The structured component bears a striking resemblance to the ligand localized $\pi-\pi^*$ phosphorescence of bpy in $Rh(bpy)_3^{3+}$.[35a] The broad structureless emission agrees well in shape and energy to MLCT emissions of other Re(I) complexes.[16] Thus, we assign the structureless emission to an MLCT transition and the structured one to a ligand-localized $\pi-\pi^*$ phosphorescence. Lifetime data (vide infra) support these assignments.

The relative amounts of ligand and CT emission depend on the excitation wavelength. Excitation at 410 nm relative to 350 nm

(41) Allsop, S. R.; Cox, A.; Kemp, T. J.; Reed, W. J. *J. Chem. Soc., Faraday Trans. 1* 1978, *74*, 1275.
(42) (a) Crosby, G. A. *Acc. Chem. Res.* **1975**, *8*, 231. (b) Cook, M. J.; Lewis, A. P.; McAuliffe, G. S. G.; Sharda, V.; Thompson, A. J.; Robbins, D. J. *J. Chem. Soc., Perkin Trans. 2* **1984**, *1303*.
(43) Mandal, K.; Pearson, T. D. L.; Krug, W. P.; Demas, J. N. *J. Am. Chem. Soc.* **1983**, *105*, 701.

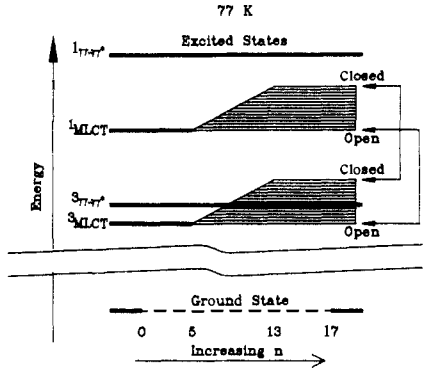

Figure 11. 77 K excited-state diagram for the zero-point energy of the lowest states of $Re(bpy)(CO)_3NC(CH_2)_nCH_3^+$ as a function of n. The band of energies represents a range of possible frozen conformations. States of molecules with the same conformation are connected by arrows.

very much favors the CT emission. For 410-nm excitation, it is clear that the CT emission energy depends on n; larger n's move the broad CT emission band to higher energy. This is consistent with our assignment of the structureless emission as being CT in character; the CT absorptions and emissions blue shift with increasing n at room temperature.

We attribute the variations in emission spectra as arising from the presence of different conformational forms of the complex. We suggest that the forms differ in the degree of fold back of the alkyl chain onto the bpy. Little or no fold back favors MLCT emission (n = 0–5), and a high degree of fold back favors $\pi-\pi^*$ phosphorescence. This is consistent with the increasing degree of fold back with increasing n observed at room temperature.

There is no doubt a variety of conformers with differing degrees of fold back and differing configurations for the same degree of fold back. In the rigid glass, each conformation is locked in place during the decay and can give rise to its independent emission(s). All of our low-temperature data can be explained on the basis of the following model.

We assume that there are predominantly two types of emitting species present. One form is an open structure where the alkyl chain shows little or no fold back and gives predominantly a MLCT emission. The second forms are closed structures with a high degree of fold back. Folded species, where the hydrocarbon can interact with the bpy, push the lowest CT state to higher energy. The more extensive the overlap of the alkyl chain, the higher the CT state energy. As the CT state energy increases relative to the $^3(\pi-\pi^*)$ state, ligand phosphorescence increases relative to the CT emission.

Within the closed forms there is no doubt a continuum of different conformers, each with a different degree of interaction with the π-cloud of the bpy and a different degree of $\pi-\pi^*$ to MLCT emission. With increasing n the closed structures become progressively more favored, and, thus, the ratio of $\pi-\pi^*$ to MLCT emission increases.[44]

We show this model schematically in Figure 11. Only the *zero-point state energies* are shown, and higher vibrational bands of each state are omitted for clarity. It should be recognized that above the zero-point energy, each state will absorb. For example, excitation into the $^1(\pi-\pi^*)$ will also yield excitation of the lower ^{1}CT state; see the absorption spectra of Figure 1. The band in CT energies arises from the range of conformations and the sensitivity of the CT state energies to local environment. To clarify that each point in the band corresponds to a different conformation of the same molecule, we have drawn two double-headed arrows showing which ^{1}CT and ^{3}CT states belong to the same conformation. Conformational changes should have minimal effect on the energy of the $\pi-\pi^*$ states because there is no large dipole moment change upon excitation. This is supported experimentally by the invariance of the $\pi-\pi^*$ phosphorescence peaks for complexes with different n's.[45]

We turn now to the reason for the excitation wavelength dependence of the emission spectra. For the lower excitation energies ($\geq$350 nm), excitation is directly and virtually exclusively into a ^{1}CT state; the ligand-localized singlet states do not absorb at all in this region, and the absorption of the ligand-localized triplet is too small to be excited directly. For higher energy excitation, excitation is into both the ^{1}CT and the $^1(\pi-\pi^*)$ states, although the absorption spectra suggest that 320 nm predominantly excites the $^1(\pi-\pi^*)$ state and 275 nm excites efficiently the CT state. See Figure 1. Yet, for each n there are no discernible differences in the 77 K emission spectra for 275-, 320-, and 350-nm excitation. There are two plausible reasons for the wavelength effects.

The first explanation is that we are simply photoselecting different conformers with different absorption spectra. Low-energy excitation (>350 nm) selectively excites ^{1}CT states of open forms that have the ^{3}CT state lowest; this yields predominantly CT emissions. Excitation at higher energies in the ^{1}CT manifold can excite ^{1}CT absorptions of both open and closed forms. Depending on the degree of fold back, these can have either the ^{3}CT or $^3(\pi-\pi^*)$ states lowest, which will yield largely CT or ligand emissions, respectively. Still deeper UV excitation will give mixed ^{1}CT and $^1(\pi-\pi^*)$ excitation with little discrimination of the different forms. Thus, higher energy excitation will give mixed CT and $\pi-\pi^*$ phosphorescence.

The second explanation is suggested by the sharpness of the transition from CT to mixed CT $\pi-\pi^*$ emission and the invariance of the ratio with wavelength ($\leq$320 nm). It is possible that there is a state crossing from the ^{1}CT to the $^3(\pi-\pi^*)$ manifold at an energy well above the zero-point energy of the ^{1}CT state. Below this crossing energy only the ^{1}CT manifold is excited and CT emission dominates. Excitation at any point above this state crossing yields the same ratio of ligand to CT emission. This implies that the relaxation paths in the excited-state manifold all proceed directly through the ^{1}CT state with the crossing, and there is little crossing into the $^3(\pi-\pi^*)$ below this point.

We cannot currently discriminate between these two models. However, because of the sensitivity of the absorption spectra to fold back, some photoselection must be occurring. Further work to assess the details of the excitation wavelength effect on the emission spectra are in progress.

Low-Temperature Luminescence Lifetimes. The nonexponential 77 K luminescence decay curves are successfully fit by a double-exponential decay (Table II). If the two emissions are completely independent, $K_i\tau_i$ is the total emission contribution from each component. The fractional contribution of the long-lived emission to the total emission at each monitored wavelength is given in eq 6.

$$f_l = K_l\tau_l/(K_s\tau_s + K_l\tau_l) \quad (6)$$

There is clearly a short-lived 5–8-μs component and a rather long-lived 15–25-μs component in all cases. While there is a suggestion that the τ's may vary with complex and monitoring wavelength, our precisions are too poor to be certain.

The fractional contribution of the long-lived component, f_l, is largest when we monitor at the wavelength of the $\pi-\pi^*$ phosphorescence, and the short-lived contribution maximizes when we

(44) A model that assumes exclusively one type of emission from the open and one from the closed forms is inadequate. It predicts that there can only be two emissions present in all the spectra: the structured $\pi-\pi^*$ phosphorescence and the broad MLCT spectrum of the open noninteracting form (n = 0–5). The continuous shift of the CT emission with increasing n for 410-nm excitation (Figure 4B) reveals clearly that closed forms can also give rise to MLCT emissions and that the CT emission spectrum depends on the degree of fold back. Thus, we conclude that different forms can give rise to dual emissions. This is not unreasonable since the n = 0 and n = 5 complexes both show evidence for dual emissions even though they cannot exhibit different degrees of alkyl chain fold back onto the bpy.

(45) It would not be unreasonable to expect different closed conformers to show different τ's. Our low-temperature τ data support this by suggesting that the τ's of the CT and $\pi-\pi^*$ emissions may depend slightly on n, but our uncertainties are too large to make a definitive statement.

monitor in a region dominated by the CT emission. Thus, we assign the 4-8-μs component to a predominately MLCT emission while the longer lived component is largely $^3(\pi-\pi^*)$ in character.

The observed $\pi-\pi^*$ phosphorescence τ's are quite short compared to the millisecond τ's observed for the purer $^3(\pi-\pi^*)$ phosphorescences for RhL_3^{3+} species.[17] The shortness of our ligand decays arise from spin-orbit coupling mixing the ligand $^3(\pi-\pi^*)$ with allowed states such as the MLCT states.[46] Mixing will introduce more singlet character into the ligand triplet state, make the ligand phosphorescence more allowed, and shorten its lifetime.

The increase in f_l and K_l/K_s with increasing n confirms the steady-state emission results and shows that increasing n increases the $\pi-\pi^*$ phosphorescence. This is consistent with our interpretation that the fraction of closed form conformers increases with n.

We turn now to a comparison of the room-temperature and 77 K models of Figures 10 and 11. In both cases for long chains some of the conformers invert the ordering of the MLCT and $\pi-\pi^*$ states. The differences in emission parentage arise from the fact that at room temperature the initially excited CT state can lose substantial amounts of energy by solvent reorganization around the new dipole formed in the excited state. This leads to the effective collapse of the band (Figure 11) to a single thermally equilibrated (thexi) state that is the lowest excited state in the molecule. In room-temperature fluid media, this reorganization can occur in a time scale short compared to τ. Thus, excitation of a conformation that would initially have the ^{3}CT state higher than the $^3(\pi-\pi^*)$ state will promptly relax to a state where the ^{3}CT state is lower and from which the emission will arise.

In rigid glasses, however, the relaxation time is long compared to τ, and the CT states cannot relax rapidly. Under these conditions, if the excited conformer has the ^{3}CT state above the $^3(\pi-\pi^*)$ state, this ordering will persist and ligand-localized emission will dominate.

(46) We can exclude shortening of the τ by either kinetic interconversion to the more allowed MLCT state or shortening of lifetime by a low-emission yield. In both cases the Φ_{em}'s would have to be quite low to explain the data, but the yields are much too high. The already high 298 K Φ_{em}'s are increased substantially on cooling to 77 K.

Conclusions

We report a unique intramolecular perturbation of an excited-state manifold by a normally passive alkyl chain. Intramolecular fold back, a strong function of chain length, alters the solvent environment around the excited portion of the molecule with a concomitant change in the state energies and decay paths. Our results suggest that the alkyl chain can function as a molecular switch and invert the lowest excited states in the molecules at low temperature. We suggest that the close proximity of the CT and ligand-localized states of these complexes coupled with the high sensitivity of the CT state energy to its microenvironment accounts to a considerable degree for the large inter- and intramolecular effects observed. The very high environmental sensitivity of these molecules and the ease of making structural modifications suggest their application as site-selective probes of local microstructure in organized media and in biological macromolecules. Further work is in progress.

Acknowledgment. We gratefully acknowledge support by the National Science Foundation (Grant CHE 86-00012) and the American Cancer Society (Grant IN-149B). All lifetime measurements were carried out at the University of Virginia laser facility in part with National Science Foundation Grant CHE 77-09296. We also gratefully acknowledge Hewlett-Packard for the gift of the 8450A spectrophotometer and Henry Wilson for his kind assistance.

Registry No. α-CD, 10016-20-3; β-CD, 7585-39-9; $(bpy)Re(CO)_3Cl$, 55658-96-3; $[(bpy)Re(CO)_3NCCH_3]^+$, 62972-14-9; $[(bpy)Re(CO)_3NC(CH_2)_2CH_3](ClO_4)$, 114597-22-7; $[(bpy)Re(CO)_3NC(CH_2)_5CH_3](ClO_4)$, 114614-26-5; $[(bpy)Re(CO)_3NC(CH_2)_7CH_3](ClO_4)$, 114597-23-8; $[(bpy)Re(CO)_3NC(CH_2)_9CH_3](ClO_4)$, 114597-24-9; $[(bpy)Re(CO)_3NC(CH_2)_{10}CH_3](ClO_4)$, 114597-25-0; $[(bpy)Re(CO)_3NC(CH_2)_{13}CH_3](ClO_4)$, 114614-27-6; $[(bpy)Re(CO)_3NC(CH_2)_{17}CH_3](ClO_4)$, 114597-26-1; O_2, 7782-44-7.

Supplementary Material Available: Preparation of $[(bpy)Re(CO)_3NC(CH_2)_nCH_3](ClO_4)$ and tables of elemental analytical data, electronic UV-visible absorption data, solvent sensitivity, emission spectral data, solvent dependence, excited-state lifetimes, and oxygen-quenching rates (8 pages). Ordering information is given on any current masthead page.

Reactions of Polypyridylchromium(II) Ions with Oxygen: Determination of the Self-Exchange Rate Constant of O_2/O_2^-

Khurram Zahir, James H. Espenson,* and Andreja Bakac*

Contribution from the Ames Laboratory and Department of Chemistry, Iowa State University, Ames, Iowa 50011. *Received December 17, 1987*

Abstract: Reductive quenching of the ^{2}E excited states of CrL_3^{3+} complexes, where L is 2,2'-bipyridine (bpy), 1,10-phenanthroline (phen), and their substituted analogues, by disodium ethylenediaminetetraacetate and sodium oxalate was studied by use of laser flash photolysis. The quenching by both compounds results in the rapid, irreversible formation of CrL_3^{2+} with a quantum yield that can approach a value of 2.0. This novel method for the generation of CrL_3^{2+} was utilized to study the reactions of CrL_3^{2+} with ground-state dioxygen. The rate constants for these reactions show a linear dependence on ΔG° as predicted by Marcus theory and range from 2.5×10^5 M^{-1} s^{-1} ($Cr(5\text{-}Clphen)_3^{2+}$) to 2.5×10^7 M^{-1} s^{-1} ($Cr(Me_2phen)_3^{2+}$). It is postulated that the reactions proceed by outer-sphere electron transfer to yield superoxide ion as the initial product, as supported by the quantity of H_2O_2 determined after its disproportionation. The electrostatically corrected Marcus cross-relation yielded $k_{22} = 2 \pm 1$ M^{-1} s^{-1} for the self-exchange rate constant of the O_2/O_2^- couple. A close inspection of the data obtained in this work along with the literature data strongly suggests that the true value of k_{22} lies in the range 1-10 M^{-1} s^{-1}.

Since the discovery of superoxide dismutase by McCord and Fridovich[1] in 1968, there has been a great deal of interest in the chemistry of superoxide.[2-5] One such area of interest relates to the electron-transfer reactions of dioxygen and superoxide with

0002-7863/88/1510-5059$01.50/0